Surface stopping

S. Peter Apell
Departamento de Física de Materiales, Facultad de Ciencias Químicas, Universidad del Pais Vasco, Euskal Herriko Unibertsitatea, Apartado 1072, San Sebastian 20080, Spain

John R. Sabin and S. B. Trickey
Quantum Theory Project, Department of Physics, University of Florida, Gainesville, Florida 32611-8435
(Received 7 August 1996; revised manuscript received 31 March 1997)

Detailed, materials-specific stopping calculations for ultrathin films exhibit a scaling with layer number N which would be expected for asymptotic N but not small N's: a bulk contribution plus a term linear in $1/N$ fit the calculations extremely well. We derive this scaling for a jellium model with a general spatially varying density profile. The model gives the magnitude of the $1/N$ term correctly as well as the scaling with kinetic energy of that contribution to the stopping. We also show that the loss to surface excitations is larger than the $1/N$ term for $v \geq 0.7$ (atomic units) and calculate the projectile velocity dependence of the apparent position of the surface plane. [S1050-2947(97)05410-3]

PACS number(s): 34.50.Bw, 61.80.Az

I. INTRODUCTION

Historically the study of stopping power has focused primarily on the phenomenon in bulk crystals or extremely dilute gases [1]. However, with increased experimental resolution, refined theoretical tools, rapid development of materials processing, and the even more rapid emergence of very thin layered materials as critical elements of microelectronic technologies, the study of energy deposition in condensed systems can be expected to follow the trend of condensed matter physics and materials science, namely, a broadening of focus to include surface and film phenomena.

Detailed, predictive, materials-specific calculations on ordered ultrathin films (UTF's) have, of course, been a staple of surface science for some time. The original motivation was to model crystalline surfaces by treating N layers with N as large as computationally feasible. A modest subset of such calculations (for our own work with co-workers see Refs. [2–9]) has focused on characterizing and understanding the intrinsic features expected to arise in UTF's on account of their unique combination of nanostructure in one dimension and translational order in the other two. Experimental investigation of such systems is still rather rare; for an example see Ref. [10].

Electronic stopping in a finite solid (including a UTF) is an integrated measure of the excitation spectrum involving both bulk and surface contributions. The excitation spectrum in turn depends on the screening in the material and its aggregation state, i.e., on the details of bonding and structure. Stopping is therefore an indirect, non-thermochemical measure of bonding in a solid or UTF. This dependence is most clearly illustrated by the difference in metallic and insulating response to an external or internal electronic perturbation. Experimentally [11–12], as well as theoretically [13–14], electronic stopping is found to decrease with increased bonding, a relationship clearly seen for a solid in different aggregation forms, the so-called phase effect [13,15]. (Such behavior is, of course, consistent with predictions by the early investigators of stopping, e.g., Bohr [16] and Bethe [17].)

The findings by Rose *et al.* [18] that binding is a universal feature, manifested in generic binding energy relations for such disparate systems as diatomic molecules, metallic adhesion, cohesion, and chemisorption, leads one to ask if stopping shows similar universal features. Particular issues include whether stopping reflects the detailed surface reconstruction or relaxation of a UTF and whether there are intrinsic surface effects to be seen in stopping for periodic systems with a finite characteristic dimension. The answer from detailed calculations based on all-electron, full-potential density functional theory (DFT) calculations is affirmative. However, while those calculations make predictions of great detail and precision, their formal and computational complexity makes it difficult to see the physical underpinnings of the systematics in the results.

Specifically, a series [6,8] of recent calculations [19–21] shows a remarkable and simple systematic behavior [22]. Within the estimated precision of the calculations, the calculated electronic stopping $S(N,v)$ for a sequence of N layers ($N \leq 4$) and projectiles of velocity v (for v above the stopping curve maximum where Bethe theory should be valid) can be written as

$$S(N,v) = S(\infty,v) + \frac{1}{N} S_L(v). \tag{1}$$

This relation holds for Li, diamond (unrelaxed), and graphite UTF's [with different values of $S(\infty,v)$ and $S_L(v)$, obviously]. See representative Figs. 1 and 2 for the Li N layer.

Such behavior would be expected for $N \to \infty$, in which case the constant term would be the bulk crystalline stopping cross section at the specified projectile velocity and the coefficient of the linear term would be the surface correction for a semi-infinite crystal. Rather less expected is that the constant coefficient from a fit to the *small-N* UTF results is consistent with the crystalline cross section. Furthermore, this linear scaling of S with $1/N$ for small N tracks the well-known scaling behavior of the cohesive energy of UTF's: the constant term is the bulk cohesive energy and the $1/N$ term is

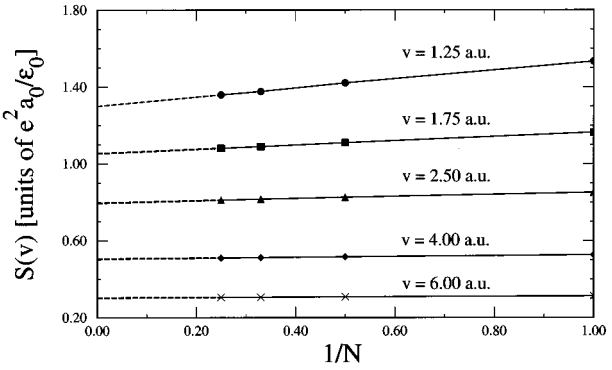

FIG. 1. Stopping cross section for a proton of velocity v versus the reciprocal layer number for N layers of lithium. All projectile velocities are above the maximum in the stopping curve, where the Bethe theory used in these calculations should be valid. Notice the linearity of the plot. Whereas this linearity could be anticipated for large N, recent calculations show that it is also true for a thin system. Shown dotted is the extrapolation to the ''bulk'' result which is within $\approx 10\%$ of standard bulk calculations [40]. The stopping is given in units of $e^2 a_0/\epsilon_0$ (9.58×10^{-15} eV cm^2/atom).

the surface energy [23]. The appeal, by analogy with the energetic behavior, is to interpret the two stopping terms from the UTF's as the bulk and surface contributions but the underlying physics remains a question.

While experimental technology is just beginning to approach the sophistication necessary to prepare an unsupported UTF (and the resolution necessary to measure its energy loss spectra), detailed calculations of stopping by unsupported UTF's have been around for some time [5–9]. From the perspective of attempting to develop a qualitative or semiquantitative interpretive model, it is actually advantageous to be able to compare the model with such theoretical calculations first. Those calculations have well-defined conditions and approximations, as contrasted with real experimental findings which are bound to involve more complications and which in principle are not necessarily results of a general nature but rather specific findings for a particular combination of target material and preparation.

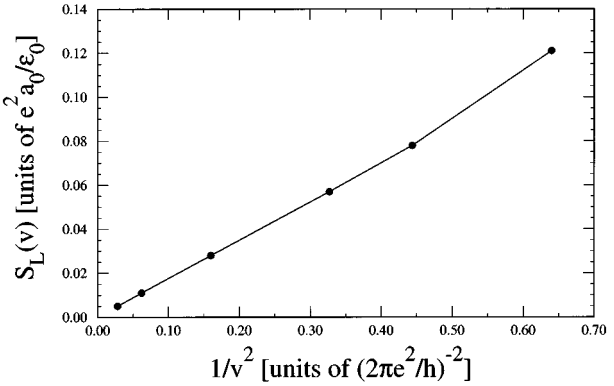

FIG. 2. The slope $S_L(v)$ versus the inverse kinetic energy of the projectile; note the almost exact linearity. Also notice the order of magnitude difference with respect to the total stopping cross section. $S_L(v)$ is in units of $e^2 a_0/\epsilon_0$ (9.58×10^{-15} eV cm^2/atom) and v is in atomic units.

As we show here, stopping in a thin film does show universal (in the sense of generic) aspects and does distinguish simple bulk relaxation at a surface from genuine surface effects [22] in ways which are interpretable via a clear physical model. The approach taken is to analyze the surface contribution to stopping for a semi-infinite medium, then extend the results to a model UTF.

II. QUALITATIVE FEATURES

The Bethe theory for stopping, used here as well as being the basis for the theoretical calculations to which we compare [5–9,22], usually is conceptualized in terms of a bulk target. Bethe theory gives the linear energy loss $-dE/dz$ of an energetic ion in matter as (SI units)

$$-\frac{1}{\tilde{n}}\frac{dE}{dz}=S(v)=\frac{Z_1^2 Z_2 e^4}{4\pi m v^2 \epsilon_0^2}L(v), \tag{2}$$

where $\tilde{n}$ is the number density of scatterers, $S(v)$ and $L(v)$ are the stopping cross section and stopping number per scatterer, respectively, v the velocity of the incident particle, E its energy, z its path length, Z_1 the projectile charge, and Z_2 the number of electrons per target atom.

The Coulomb interaction between the projectile and the target electrons, which is fundamental to Eq. (2), evidently has no explicit reference to the presence of macroscopic boundaries (surfaces) [24]. Rather, such macroscopic contributions arise from effects upon the electron distribution and electron response. In a bulk sample terminated by a surface (a semi-infinite solid) one expects two main effects to modify the bulk stopping (S_B). One is that the sheer existence of a surface, however simple, brings in new excitations which can contribute a genuine surface part (S_S) to stopping. Whereas S_B should be independent of system size (as measured by some scale length ℓ), S_S should be dependent upon ℓ and, as well, proportional to the number of surfaces present. The other effect is that the specific form (denoted hereafter by subscript F) of the surface may alter the numerical values of the terms which arise from the simple presence (donated hereafter by subscript P) of bulk and surfaces. We therefore may conjecture the separation

$$S=S_B+S_S, \tag{3}$$

with an explicit distinction between general (i.e., simple presence) and specific (i.e., form) contributions

$$S_B=S_{BP}+S_{BF} \tag{4}$$

and

$$S_S=S_{SP}+S_{SF}. \tag{5}$$

These equations are derived in Sec. III for a jellium slab model with a nonconstant density profile along the axis perpendicular to the slab face(s). S_{BP} is the bulk stopping for an infinite system while S_{BF}, a focus of this paper, is the modification to S_{BP} induced by the form of the bulk, i.e., by the fact that the bulk is bounded by a surface. In contrast, S_{SP} is a measure of the surface loss attributable to surface excita-

tions while S_{SF} measures the modification of stopping contribution from those excitations which are traceable to the actual form of the surface.

Evidently the division between the terms in S_B and S_S, respectively, is dependent on the actual definition of the existence and form of a boundary. The simplest intuitively appealing model for a surface with well-defined meaning would be a sharp step function demarking an abrupt change from matter to vacuum. No true surface, of course, is so sharp, a fact accounted for in this work by use of a simple unidirectional profile. As a matter of convention, we shall choose to have the lowest-order contribution caused by the nonconstancy of that profile constitute S_{BF}. The remaining contributions can be sorted conveniently into those from a step-function surface, S_{SP} and the rest, which constitute S_{SF}. A test of the consistency of these identifications is provided by the fact that introduction of a surface creates new channels for excitation whose oscillator strength comes at the expense of the infinite bulk excitations. Thus it has been known for a long time that the bulk plasmon loss in a material slab has less strength than in an infinite solid by an amount which exactly balances the excitation strength of the introduced surface plasmon losses; this is the so-called *begrenzung* effect [25].

As an aside, notice that for a monolayer, which has no proper interior, there is nonetheless a bulk contribution and a surface correction in the sense that the conjectured decomposition is valid and therefore the associated, characteristic velocity dependences occur. Evidently the numerical values of the coefficients of those terms are not the same as for a thick slab. It should also be evident that because the monolayer atoms are bound to neighbors the equilibrium monolayer and atomic (dilute gas) stopping must differ [26].

III. THEORY

In the Bethe theory [17] for the mean energy loss per path length of a light ion, the stopping number is [27]

$$L(v)=\ln\frac{2mv^2}{I} \tag{6}$$

(where the projectile velocity is presumed to be sufficiently high as to make the logarithm non-negative). Materials-specific information is contained in the mean excitation energy I determined by [27]

$$\ln I=\frac{2}{\pi\omega_p^2}\int_0^\infty d\omega\,\omega\ \mathrm{Im}[-1/\epsilon(\omega)]\ln\hbar\omega \tag{7}$$

in the linear response approximation. $\mathrm{Im}[-1/\epsilon(\omega)]$, with $\epsilon(\omega)$ the long-wavelength limit of the microscopic dielectric function of the solid (assuming homogeneity), characterizes the entire electron excitation spectrum. In the plasmon pole approximation [that is, $\epsilon(\omega)$ entirely described by a collective mode at ω_p], $\mathrm{Re}\,\epsilon(\omega_p)=0$ and $\mathrm{Im}[-1/\epsilon(\omega)]=(\pi/2)\omega\delta(\omega-\omega_p)$ for ω positive. Then $I=\hbar\omega_p$ and Eq. (2) reads

$$S_B=\frac{Z_1^2Z_2e^4}{4\pi mv^2\epsilon_0^2}\ln\frac{2mv^2}{\hbar\omega_p}. \tag{8}$$

In what follows it is convenient to measure S and other quantities in Hartree atomic units. Then the reference stopping power is $s_0=e^2a_0/\epsilon_0\simeq 9.58\times10^{-15}$ eV cm^2/atom. For proton stopping ($Z_1=1$) *normalized to the number of electrons* (hence Z_2 is divided out), Eq. (8) becomes

$$S_B/s_0=\frac{1}{v^2}\ln\frac{2v^2}{\omega_p}. \tag{9}$$

Note that this is a bulk quantity (subscript B) because it is determined entirely by properties defined with respect to the bulk (though not necessarily evaluated for the bulk; see below), namely, the long wavelength dielectric function and, hence, the bulk plasmon frequency.

The usual electron gas model of a semi-inifinite slab is an electron number density profile $n(z)$ with complete translational invariance in the x-y plane and a step-function jellium background of number density ρ_B. The behavior of the model UTF will be deduced from this surface model. For convenience, denote by $n_0(z)$ the electron number density normalized to unity for the assumed bulk density

$$n_0(z)=\frac{n(z)}{\rho_B}. \tag{10}$$

From classical electromagnetism the power loss due to ion transit is just the integrated product of the ion current and the gradient of the induced potential, that is,

$$\frac{dE}{dt}=-\int d^3r\rho^{\mathrm{ion}}(\vec r,t)\vec v\cdot\vec\nabla\Phi^{\mathrm{ind}}(\vec r,t), \tag{11}$$

whence it follows immediately for constant ion velocity $\vec v=v_z\hat z$ that

$$\frac{dE}{dz}=-\int^{v_z}d^3r\rho^{\mathrm{ion}}(\vec r,t)\frac{d\Phi^{\mathrm{ind}}}{dz}(\vec r,t). \tag{12}$$

The induced potential

$$\Phi^{\mathrm{ind}}(\vec r,t)\equiv\Phi^{\mathrm{ind}}(1,t) \tag{13}$$

is the screened Coulomb interaction from the ion reduced by the external potential. In frequency-dependent (time-Fourier-transformed) form it reads

$$\Phi^{\mathrm{ind}}(1,\omega)=\int d2d3v(1,2)\epsilon^{-1}(2,3,\omega)\rho^{\mathrm{ion}}(3,\omega)-\Phi^{\mathrm{ext}}(1,\omega). \tag{14}$$

Here $v(1,2)$ is the bare Coulomb interaction between two charges at $1(\vec r)$ and $2(\vec r)$ and $\epsilon^{-1}(1,2,\omega)$ is the real-space, time-Fourier-transformed inverse dielectric function of the system [28]. (As usual the real parts of Fourier-transformed expressions are to be taken when appropriate to extract physically measurable quantities; $d2=d^3r'$ and $d3=d^3r''$) The local stopping power for a proton projectile with velocity unit vector parallel to the z axis is then

$$S(1,t)=-\hat v\cdot\vec\nabla_1\Phi^{\mathrm{ind}}(\vec r,t)\big|_{\text{projectile position}} \tag{15}$$

For the study of bulk and surface contributions it is enough to use the following high-frequency (and gradient) expansion of ϵ^{-1} [29,30]:

$$\epsilon^{-1}(1,2,\omega)=\delta(1,2)\frac{1}{\epsilon(1,\omega)}+\frac{1}{4\pi}\frac{1}{\epsilon(1,\omega)\epsilon(2,\omega)}\times\vec{\nabla}_1\epsilon(1,\omega)\cdot\vec{\nabla}_1 v(1,2)\cdots . \quad (16)$$

$\epsilon(1,\omega)$ denotes the local dielectric function

$$\epsilon(1,\omega)=1-\frac{\omega_p^2(1)}{\omega^2} \quad (17)$$

while the local plasma frequency is

$$\omega_p^2(1)=\omega_p^2\left[\frac{n(1)}{\rho_B}\right]\equiv\omega_p^2 n_0(1), \quad (18)$$

with ω_p^2 the bulk plasmon frequency as before. In terms of $n(1)$, Eq. (16) is an expansion to lowest order in $\vec{\nabla}n/n$.

After Fourier transforming with respect to the translationally invariant (xy) surface according to $\vec{\rho}\equiv(x,y)$ (and the corresponding $\vec{k}_\parallel$), the local stopping power is

$$S(1,t)=\int\frac{d\omega}{2\pi}\int\frac{d^2k_\parallel}{(2\pi)^2}e^{-i\omega t}e^{i\vec{k}_\parallel\cdot\vec{\rho}}S(\vec{k}_\parallel,z,\omega), \quad (19)$$

where the kernel on the rhs results from combining Eq. (14) plus Eqs. (16)–(18) in Eq. (15) to yield

$$S(k,z,\omega)=S_0(k,z,\omega)+\int dz' g(k,z,z')S_0(k,z',\omega)\times\frac{d}{dz'}\ln\epsilon(z',\omega). \quad (20)$$

Here

$$g(k,z,z',\omega)=-\frac{1}{2}\mathrm{sgn}(z-z')e^{-k|z-z'|} \quad (21)$$

and sgn(z) is 1 (-1) when z is positive (negative). $\epsilon(z,\omega)$ is the aforementioned local dielectric function, while $g(k,z,z')$ arises from the gradient of the Fourier-transformed Coulomb interaction. Furthermore we have defined

$$S_0(k,z,\omega)\equiv\frac{e^2}{v\epsilon_0}\int dz' g(k,z,z')e^{i\omega z'/v}[\epsilon^{-1}(z',\omega)-1]. \quad (22)$$

Equations (19)–(22) form the basis for the remaining treatment. It is now straightforward to show that the first term of Eq. (20) gives the contribution from a bounded bulk while the second gives a surface contribution. Evaluation of Eq. (22) with $\epsilon(z,\omega)=1-(\omega_p^2/\omega^2)n_0(z)$ [recall that $n_0(z)$ is the electron density $n(z)$, normalized to unity in the bulk], yields the following generalization of Eq. (9), viz.;

$$S_B(z)/s_0=\frac{n_0(z)}{v^2}\ln\frac{2v^2}{\omega_p\sqrt{n_0(z)}}, \quad (23)$$

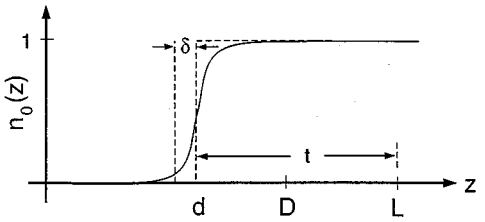

FIG. 3. Nomenclature for positions and lengths used in the Appendix. n_0 is the electron density normalized to its bulk value, d is the position of the jellium edge (one half the mean lattice spacing outside the outermost lattice plane), D is the distance at which the density profile has healed to the bulk value $[n_0(D)=1]$, δ is the apparent size of the selvage as experienced by the projectile, and $t=L-d$ is the thickness.

as might have been anticipated by letting the electron density in Eqs. (2) and (9) be replaced by $n(z)$. Equation (23) was derived earlier by Kitigawa [30] and a surface term was added in [31], but no explicit results were given.

The simple fact of a density profile causes Eq. (23) to split into two terms, hence to yield S_B Eq. (4) explicitly, as follows. Consider the total energy loss $\Delta E=\int dz S_B(z)$ for a slab of inhomogeneous electron gas with jellium thickness t given in terms of N-layer parameters as

$$t=L-d=(N-1)a_e+2\frac{1}{2}a_e=Na_e, \quad (24)$$

where a_e is the mean equilibrium interplanar distance for the N layer and the second term is to position the jellium background edge properly; see the Appendix and Fig. 3. Then, also from the Appendix,

$$S_B=S_{BP}+S_{BF}\equiv S_{BP}+\frac{1}{N}S'_{BF}, \quad (25)$$

where

$$S_{BP}/s_0=\frac{1}{v^2}\ln\frac{2v^2}{\omega_p} \quad (26)$$

and

$$S'_{BF}/s_0=\frac{1}{v^2}\frac{1}{2a_e}\mathcal{L}[n_0], \quad (27)$$

where the length functional $\mathcal{L}[n_0]$ is defined in the Appendix, Eq. (A5), as $\mathcal{L}\equiv-\int_{-\infty}^{\infty}dz n_0(z)\ln n_0(z)$. Observe first that the S_{BP} term gives the bulk behavior calculated at the mean film density. Second, the integral in S_{BF} is precisely of the form used in the orbital local plasma approximation, a key ingredient in the detailed calculations [5–9].

Note that the model automatically gives S_{BF} as inversely proportional to N as found in the calculations [22]. In fact the computed a_e values depend rather weakly upon N, especially for large N. Moreover, even though $n_0(z)$ can depend significantly on N, especially for small N, its integral divided by N is constrained by charge neutrality to be independent of N. We may conclude, therefore, that S_{BF} exhibits a $1/N$ dependence to a high degree of accuracy. We also pre-

dict from Eq. (27) that S_{BF} scales as the inverse of the kinetic energy, a behavior which is readily seen as being a prominent feature of the full calculations [22] as presented in Fig. 2.

It is essential to address the actual magnitude of S'_{BF}. To do so requires specification of the density profile. It is both convenient and physically realistic to use the universal profile given by Rose *et al.* [18]. It represents most metal surfaces if z is scaled with respect to 0.98 times the Thomas-Fermi length $\ell_{\mathrm{TF}}/a_0=\sqrt{\pi\alpha r_s/4}$, r_s being the electron gas density parameter. This means that

$$S'_{BF}/s_0=\frac{0.49}{v^2}\frac{\ell_{\mathrm{TF}}}{a_e}\mathcal{L}'[n_0]. \tag{28}$$

The quantity $\mathcal{L}'[n_0]$ is scaled to $\mathcal{L}[n_0]$ by $\mathcal{L}=0.98\ell_{\mathrm{TF}}\mathcal{L}'$ and has the value $\mathcal{L}'[n_0]=1.273$ for the Rose choice of density profile [18]. With $a_{e,N=4}=4.3$ a.u. [2] and $\ell_{\mathrm{TF}}\approx 1.15$ a.u. as appropriate for Li ($r_s=3.25$ a.u.) we get a slope for S'_{BF}/s_0 versus $1/v^2$ which is 0.167 as compared with the calculated value of 0.189. It thus appears that the main part of the slope for Li N layers is due to the genuine surface effect. A similar analysis for diamond and graphite shows not surprisingly that in those cases there are larger contributions from relaxation and effects other than the surface effect.

Alternatively, as shown in the Appendix, the width of the selvage δ (see Fig. 3) necessary to compensate for the S_{BF} term may be calculated. Note that δ is the extent to which the effective surface plane seen by the projectile moves outward as a function of incident velocity. That is, δ is the apparent surface position in that it corresponds to the position which would be assigned to the surface if all the stopping were attributed to the bulk. δ is the analog of the image plane for a charged particle outside a solid surface; the position of the image plane also depends on the energy of the particle in question, as shown by Ray and Mahan [32]. With the Rose *et al.* profile and $r_s=3.25$ a.u., δ from the Appendix, Eq. (A11), is 0.38 a.u., 0.22 a.u., and 0.18 a.u. for $v=1,2,3$ a.u. respectively. The shift outward from the nuclear surface declines smoothly with projectile velocity; see Fig. 4.

What about the explicit surface presence term in Eq. (5)? It comes from the second term in Eq. (20), which contains surface information, through $|d\epsilon(z)/dz|\propto dn_0/dz$, since $dn_0/dz\neq 0$ only in the surface region. By evaluating this term for a sharp interface and a sufficiently thick film, we find that with $S_{SP}=(1/N)S'_{SP}$,

$$S'_{SP}/s_0=\frac{\pi}{4}(\sqrt{2}-1)\frac{1}{v a_e\omega_p}. \tag{29}$$

Notice several features. First, as long as the bulk plasmon frequency and a_e are independent of N, S'_{SP} is independent of N itself. It also shows the *begrenzung* effect [25] mentioned above. The introduction of a surface having characteristic loss energies at $\omega_s=\omega_p/\sqrt{2}$ is at the expense of a reduced bulk loss (the term proportional to $\sqrt{2}-1$) above, i.e., $(\omega_s-\omega_p/2)$ [33]. See Ref. [34] for calculations of the position-dependent stopping and its contributions from bulk and surface modes, respectively, for a sharp surface. We also see that the surface term scales as $1/v$ compared to the surface term discussed earlier in this section; the latter term has a $1/v^2$ dependence.

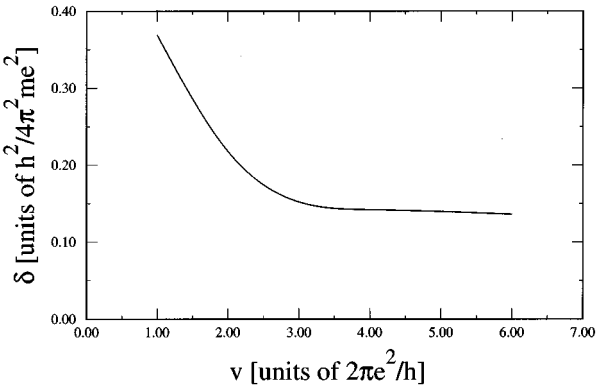

FIG. 4. Velocity dependence of the selvage δ, i.e., the effective position of the surface plane as probed by the incident proton. The classical surface position for a sharp interface (and the position of the jellium edge also) is $\delta=0$. For high velocities, all media tend toward classical response, hence $\delta\to 0$. For all $v>1$ a.u. (the validity limit on this calculation), the apparent surface is outside the classical surface.

Finally we compare the surface presence term directly with the bulk form contribution in Eq. (26); the surface correction to the bulk stopping. Formation of the ratio between the two gives

$$S_{SP}/S_{BF}=v/v_c. \tag{30}$$

v_c is given as

$$v_c/v_0\simeq\frac{2\ell_{\mathrm{TF}}\omega_p}{v_0}=\frac{2}{\sqrt{3}}\frac{1}{\alpha r_s}\approx 0.67 \tag{31}$$

for Li. This means that in the range of interest, where $v\geqslant v_0$ (v_0 is the Bohr velocity $e^2/4\pi\epsilon_0\hbar$), S_{SP} dominates clearly over S_{BF}. Thus the excitation of surface modes is more crucial to incorporate than the true surface profile when v is larger than a few atomic units. In this respect we will not calculate S_{SF} here since S_{SP} itself contains already so much that it dominates over S_{BF}.

Notice that throughout we have assumed the two surfaces to be independent of each other. In the ultrathin films this assumption is not fulfilled. For such systems the modes at the opposite surfaces couple to each other, hence change the surface loss frequencies. However, that coupling merely will change the numerical value of v_c, not its scaling with ω_p.

IV. DISCUSSION AND CONCLUSIONS

Detailed calculations of proton stopping in ultrathin films have shown a clear scaling with the inverse number of layers. Within a simple jelliumlike framework we have reproduced that behavior when it comes to the influence of the true surface on the bulk contribution. Not only does the correct velocity dependence emerge but also the absolute magnitude in the sense that the model accounts for the major part of the surface term for Lithium. Apparently the good agreement with small-N linearity arises because a bulk-like density is established at relatively low N, at least insofar as

integrals over the density are concerned. Chemically such behavior is consistent with the pervasive manifestation of different types of bonding down to remarkably small system sizes.

As an aside, the present result extends the range of properties for which periodically ordered Li exhibits jelliumlike behavior. From a textbook perspective that is a seemingly trivial statement. For certain properties, most notably the equation of state, there are large deviations (qualitative and quantitative) from free-electron-like (Thomas-Fermi-Dirac) behavior however [35]. It is therefore important to delineate the actual behavior of condensed phases of Li as distinct from the conventional wisdom about those phases.

As a system gets smaller and smaller, surface excitations should become more and more important for a charged probe coupling to the system. Our analysis shows that in fact the surface excitations give a larger contribution to the stopping power than the surface correction to the bulk result. They also scale inversely with the velocity of the projectile while the surface correction scales with the inverse square of the velocity, meaning that those surface excitations will be comparatively more important at higher velocities. The conclusion is that even if bulk terms dominate stopping in thin films down to a few layers, such calculations do need to incorporate surface losses if they are to be compared with data for real systems.

For some time to come experiment results for thin unsupported films will not be commonly available. The influence of substrates is to change the surface excitation frequencies at the interface and to smooth the surface profile there. We can still analyze experimental results within the framework outlined here provided that it is possible to account for the substrate bulk contribution by other measurements or calculations and that the genuine surface losses can be treated on a reasonable footing.

Since the focus of this paper is on the physics underlying the N-scaling behavior of stopping, we have not pursued the cohesive energy scaling issue. Note, however, that (1) both cohesive energy and stopping are related measures of the solid's excitation spectrum [36], (2) similar scaling without higher order terms in $1/N$ is present for the cohesive energies of sodium clusters down to four atoms in size [37–38], and (3) there is evidence (in the form of so-called *glue* models [39]) that much of the energetics of metallic cohesion can be accounted for on the basis of coordination. Finally, it is a well-defined procedure from thin film calculations of surface energies to extract the bulk cohesive energy from a small N calculation, the same way as we inferred $S(\infty,v)$ above [23(b)]. Thus we can suggest the analogous procedure as an interesting and efficient way of calculating bulk stopping power while at the same time obtaining the surface effects, all from one calculation.

ACKNOWLEDGMENTS

We acknowledge many helpful discussions with Richard J. Mathar and with members of the energy deposition group at the Basque University, San Sebastian. We thank P. Sigmund for a careful reading of a much earlier version of the manuscript. S.P.A. and J.R.S. acknowledge support from the Swedish National Science Research Council. J.R.S. and S.B.T. were supported in part by the U.S. Army Office of Research.

APPENDIX

Consider the energy loss for depth $L \geqslant D$ (see Fig. 3 for notation) into a semi-infinite jellium slab system such that

$$n_0(z)=1 \quad \forall z \geqslant D, \tag{A1}$$

with the origin sufficiently far from the jellium edge at $z=d$ that the electron charge density for all $z \leqslant 0$ is zero. Let

$$\Delta E \equiv \int dz S(z)/s_0 . \tag{A2}$$

Add and subtract the jellium background of density $\rho_B \theta(z-d)$, where $\theta(z)$ is unity for z positive and zero otherwise. Because of the limiting behavior of the density and charge neutrality $n_0(0)=0$, $n_0(L)=1$, $\int_0^L dz[n_0(z) - \theta(z-d)]=0$, we get

$$\Delta E(L)=\frac{1}{v^2}\int_0^L dz \ln\frac{2v^2}{\omega_p}\theta(z-d) - \frac{1}{2v^2}\int_{-\infty}^{\infty} dz n_0(z)\ln n_0(z). \tag{A3}$$

Notice that the second term is the surface-confined contribution while the first behaves as a bulk contribution. Immediately one has

$$\Delta E(L)=\frac{1}{v^2}\ln\left[\frac{2v^2}{\omega_p}\right](L-d)-\frac{1}{2v^2}\int_{-\infty}^{\infty} dz n_0(z)\ln n_0(z) = \frac{1}{v^2}\ln\left[\frac{2v^2}{\omega_p}\right](L-d)+\frac{1}{2v^2}\mathcal{L}[n_0], \tag{A4}$$

where $\mathcal{L}$ is a length characteristic of the electron density profile neutralization, which is given by

$$\mathcal{L}[n_0] \equiv -\int_{-\infty}^{\infty} dz n_0(z)\ln n_0(z). \tag{A5}$$

Two choices for the length scale of energy deposition can be distinguished readily within the model. One is with respect to the jellium edge. Then one has

$$S(L,v) \equiv \Delta E/(L-d) \equiv S_{BP}+S_{BF}, \tag{A6}$$

where, from Eq. (9),

$$S_{BP}/s_0=\frac{1}{v^2}\ln\frac{2v^2}{\omega_p} \tag{A7}$$

and

$$S_{BF}/s_0=\frac{1}{v^2}\frac{1}{2(L-d)}\mathcal{L}[n_0], \tag{A8}$$

with $s_0\equiv e^2a_0/\epsilon_0=h^2/\pi m$ as before. If now the electron profile is of some finite thickness t, symmetric in its transverse axis, and obeys a corresponding charge neutrality condition at the center, the same expressions result, except that $t=L-d$. To connect the model with a UTF of mean interplanar spacing a_e, recall that the jellium edge is set a distance $a_e/2$ outside each of the UTF faces, whence $t=T+2(a_e/2)$ with T the distance between the exterior-most nuclear planes.

Alternatively, the length scale for energy deposition can be chosen to include the selvage δ explicitly [9]. Since both it and the term in $\Delta E(L)$ which depends on $\mathcal{L}[n_0]$ measure the contribution to stopping caused by the deviation of the profile from a step function, δ can be adjusted within the model to cancel $\mathcal{L}$, hence yield an effective, velocity-dependent jellium edge position. One has

$$\mathcal{S}(L,v)\equiv\Delta E/(L-d+\delta)=S_{BP}\frac{(L-d)}{(L-d+\delta)}+\frac{1}{v^2}\frac{1}{2(L-d+\delta)}\mathcal{L}[n_0]. \tag{A9}$$

Therefore, to lowest order in δ, the fraction of S_{BP} which offsets the $\mathcal{L}$ term follows from requiring that

$$\delta S_{BP}(v)=\frac{\mathcal{L}[n_0]}{2v^2}. \tag{A10}$$

For $S_{BP}(v)>0$, that is, $2v^2/\omega_p>1$, this relationship becomes

$$\delta=\frac{\mathcal{L}[n_0]}{2\ln(2v^2/\omega_p)}. \tag{A11}$$

Note that δ is used here as a width, $\delta\geqslant 0$.

[1] See, e.g., recent overview by P. Sigmund, Nucl. Instrum. Methods Phys. Res. B **85**, 541 (1994).

[2] J. C. Boettger and S. B. Trickey, Phys. Rev. B **45**, 1363 (1992).

[3] J. Z. Wu, S. B. Trickey, J. R. Sabin, and J. C. Boettger, Phys. Rev. B **51**, 14 576 (1995).

[4] J. C. Boettger, U. Birkenheuer, N. Rösch, and S. B. Trickey, Phys. Rev. B **52**, 2025 (1995).

[5] J. Z. Wu, S. B. Trickey, J. R. Sabin, and D. E. Meltzer, Nucl. Instrum. Methods Phys. Res. B **56/57**, 340 (1991).

[6] J. Z. Wu, S. B. Trickey, and J. R. Sabin, Nucl. Instrum. Methods Phys. Res. B **79**, 206 (1993).

[7] J. Z. Wu, S. B. Trickey, and J. R. Sabin, Int. J. Quantum Chem. **S-27**, 219 (1993).

[8] J. Z. Wu, S. B. Trickey, and J. R. Sabin, Int. J. Quantum Chem. **S-28**, 299 (1994).

[9] S. B. Trickey, J. Z. Wu, and J. R. Sabin, Nucl. Instrum. Methods Phys. Res. B **93**, 186 (1994).

[10] A. Nagashima, N. Tejima, Y. Gamou, T. Kawai, and C. Oshma, Phys. Rev. Lett. **75**, 3918 (1996).

[11] W. Meckbach and S. K. Allison, Phys. Rev. **132**, 294 (1983).

[12] P. Bauer, F. Kastner, A. Arnau, A. Salin, P. D. Fainstein, V. H. Ponce, and P. M. Echenique, Phys. Rev. Lett. **69**, 1137 (1992).

[13] J. Oddershede, J. R. Sabin, and P. Sigmund, Phys. Rev. Lett. **51**, 1332 (1983).

[14] A. Arnau, P. Bauer, A. Salin, F. Kastner, V. H. Ponce, P. D. Fainstein, and P. M. Echenique, Phys. Rev. B **49**, 6470 (1994).

[15] P. Bauer, F. Kastner, A. Arnau, A. Salin, V. H. Ponce, and P. M. Echenique, J. Phys.: Condens. Matter **5**, A273 (1993).

[16] N. Bohr, Philos. Mag. **25**, 10 (1913).

[17] H. Bethe, Ann. Phys. (Leipzig) **5**, 325 (1930).

[18] J. H. Rose, J. R. Smith, and J. Ferrante, Phys. Rev. B **28**, 1835 (1983).

[19] The calculations of Refs. [3], [6], and [8] assumed a proton at normal incidence with effects of channeling and changes in projectile charge state neglected. Sigmund's kinetic theory of stopping (see Ref. [20]) is used, with the stationary target stopping number required therein obtained from the Bethe theory, in an explicitly orbital-dependent formulation. The orbital local plasma approximation (see Ref. [21]) was used; the local density approximation to DFT was the source of all required inputs.

[20] P. Sigmund, Phys. Rev. A **26**, 2497 (1982).

[21] D. E. Meltzer, J. R. Sabin, S. B. Trickey, and J. Z. Wu, Nucl. Instrum. Methods Phys. Res. B **82**, 493 (1993).

[22] S. P. Apell, J. R. Sabin, and S. B. Trickey, Int. J. Quantum Chem. **S29**, 153 (1995); see also S. B. Trickey and J. C. Boettger, in *Condensed Matter Theories*, edited by E. V. Ludeña and B. Malik (Nova, New York, in press), Vol. 11.

[23] (a) J. G. Gay, J. R. Smith, R. Richter, F. J. Arlinghaus, and R. H. Wagoner, J. Vac. Sci. Technol. A **2**, 931 (1983); (b) J. C. Boettger, Phys. Rev. B **49**, 16 978 (1994).

[24] S. P. Apell and D. R. Penn, Phys. Rev. B **34**, 6612 (1986).

[25] R. H. Ritchie, Phys. Rev. **106**, 874 (1957); H. Boersch, J. Geiger, and W. Stikel, Z. Phys. **212**, 130 (1968).

[26] The two cases are similar, however, in the sense that the energy loss for the N layers is very small relative to the incoming beam energy. The same experimental response to this resolution challenge that is used for dilute gas stopping measurements is available in principle for the N-layer case, namely, creation of a suitably thick target out of an assembly of the very thin ones.

[27] U. Fano, Annu. Rev. Nucl. Sci. **13**, 1 (1963).

[28] The more familiar form for the dielectric function is Fourier transformed to reciprocal space also. Whether one works in Fourier space or in direct space is a matter of convenience for the problem at hand. Since we are concerned with the contributions to stopping from the existence and shape of real-space boundaries, the direct-space representation of the dielectric function is more convenient.

[29] G. Mukhopadhyay and S. Lundqvist, Nuovo Cimento B **27**, 1 (1975).

[30] M. Kitigawa, Nucl. Instrum. Methods Phys. Res. B **13**, 133 (1986).

[31] M. Kitigawa, Nucl. Instrum. Methods Phys. Res. B **33**, 409 (1988).
[32] R. Ray and G. D. Mahan, Phys. Lett. **42A**, 301 (1972).
[33] R. Núñez, P. M. Echenique, and R. H. Ritchie, J. Phys. C **13**, 4229 (1980).
[34] R. Kawai, N. Itoh, and Y. H. Ohtsuki, Surf. Sci. **114**, 137 (1982).
[35] J. C. Boettger and S. B. Trickey, Phys. Rev. B **32**, 3391 (1985); W. G. Zittel, J. Meyer-ter-Vehn, J. C. Boettger, and S. B. Trickey, J. Phys. F **15**, L247 (1985); J. Meyer-ter-Vehn and W. G. Zittel, Phys. Rev. B **37**, 8674 (1988); J. A. Nobel, S. B. Trickey, P. Blaha, and K. Schwarz, *ibid.* **45**, 5012 (1992).
[36] R. A. Craig, Phys. Rev. B **6**, 1134 (1972).
[37] C. Brechignac, Ph. Cahuzac, F. Carlier, M. de Frutos, and J. Legnier, Z. Phys. D **19**, 1 (1991).
[38] J. Jortner, Z. Phys. D **24**, 247 (1992).
[39] D. Tománek, S. Mukherjee, and K. H. Bennemann, Phys. Rev. B **28**, 665 (1983); I. J. Robertson, V. Heine, and M. C. Payne, Phys. Rev. Lett. **70**, 1944 (1993).
[40] H. H. Andersen and J. F. Ziegler, *Hydrogen Stopping Powers and Ranges in All Elements*, Vol. 3 of *The Stopping and Ranges of Ions in Matter* (Pergamon, New York, 1977).